Naunyn-Schmiedeberg's Arch Pharmacol (1993) 347:569–582

Naunyn-Schmiedeberg's
Archives of
Pharmacology

Autoradiographic characterisation and localisation of 5-HT_{1D} compared to 5-HT_{1B} binding sites in rat brain

Anne T. Bruinvels, José M. Palacios*, and Daniel Hoyer

Preclinical Research 360/604, Sandoz Pharma Ltd., CH-4002 Basel, Switzerland

Received November 9, 1992/Accepted February 11, 1993

Summary. The regional distribution and the pharmacology of the binding sites labelled with the novel 5-hydroxytryptamine (serotonin) 5-$HT_{1B/1D}$ selective radioligand serotonin-O-carboxy-methyl-glycyl-[^{125}I]tyrosinamide (abbreviated [^{125}I]GTI for the sake of simplicity) was determined using quantitative autoradiography in rat brain. The distribution of [^{125}I]GTI binding sites was largely comparable to that of [^{125}I]iodocyanopindolol ([^{125}I]ICYP) which labels 5-HT_{1B} binding sites (in the presence of 8-OH-DPAT (8-hydroxy-[2N-dipropylamino]tetralin) and isoprenaline, to prevent binding to 5-HT_{1A} and β-adrenoceptor binding sites), although a detailed analysis revealed differences.

The pharmacology of the [^{125}I]GTI binding sites was analysed using compounds known to display high affinity for and/or distinguish between 5-HT_{1B} and 5-HT_{1D} sites: 5-carboxamidotryptamine (5-CT), sumatriptan, CP 93129 (5-hydroxy-3(4-1,2,5,6-tetrahydropyridyl)-4-azaindole), (−)pindolol, PAPP (4[2-[4-[3-(trifluoromethyl) phenyl]-1-piperazinyl]ethyl]benzeneamine), rauwolscine, and 8-OH-DPAT. The displacement of [^{125}I]GTI by 5-CT was monophasic. By contrast, the selective 5-HT_{1B} compound CP 93129 and (−)pindolol produced biphasic curves showing a majority of high affinity sites in the globus pallidus and the substantia nigra, whereas PAPP and sumatriptan (which are somewhat 5-HT_{1D} selective) produced biphasic curves indicating a minority of high affinity sites in these areas. In addition, by blocking the 5-HT_{1B} sites with 100 nM CP 93129, the remaining population of [^{125}I]GTI binding sites could be studied and was found to have high affinity for PAPP, rauwolscine and 8-OH-DPAT. The pharmacological profile of the major binding component was typical of the 5-HT_{1B} type: 5-CT > CP 93129 ⩾ (−)pindolol > sumatriptan ⩾ PAPP > rauwolscine. The profile of the minor component of [^{125}I]GTI binding is best characterised as that of a 5-HT_{1D} site: 5-CT > PAPP ⩾ sumatriptan > rauwolscine > (−)pindolol ⩾ CP 93129.

The localisation of the non 5-HT_{1B} [^{125}I]GTI binding sites was characterised by blocking the 5-HT_{1B} receptors with 100 nM CP 93129. Low densities of the 5-HT_{1D} recognition sites were found to be present in globus pallidus, ventral pallidum, caudate-putamen, subthalamic nucleus, entopeduncular nucleus, substantia nigra (reticular part), nuclei of the (normal and accessory) optic tract, different nuclei of the geniculate body and frontoparietal cortex, although higher densities of 5-HT_{1B} sites were always observed in the same structures. Thus, in agreement with the recent cloning of a rat 5-$HT_{1D\alpha}$ receptor cDNA, the presence and the distribution of 5-HT_{1D} sites could be documented in rat brain. However, when compared to 5-HT_{1B} sites, 5-HT_{1D} sites represent only a minor component of the [^{125}I]GTI binding in the rat brain structures studied.

Key words: Quantitative in vitro receptor autoradiography – [^{125}I]GTI, 5-HT_{1D} binding sites – 5-HT_{1B} binding sites – Rat brain

Introduction

The 5-hydroxytryptamine (5-HT, serotonin) receptor family is a typical example of the large diversity of receptors activated by a single neurotransmitter (Hoyer 1991). Besides the 5-HT_2, 5-HT_3 and 5-HT_4 receptor classes which have been established (Peroutka 1988; Dumuis et al. 1988), the 5-HT_1 receptor subclass was initially studied using radioligand binding techniques, and was characterised by its high affinity for [^{3}H]5-HT itself, which does not label 5-HT_2 sites (Peroutka and Snyder 1979). Subsequently, it was demonstrated by the use of spiperone that [^{3}H]5-HT binding sites were not homogeneous: spiperone differentiates between 5-HT_{1A} and 5-HT_{1B} sites (Pedigo et al. 1981). So far, at least six

* Present address: Departemento de Neuroquìmica, C.I.D., C.S.I.C., Jordi Girona 18-26, E-08034 Barcelona, Spain

Correspondence to: D. Hoyer at the above address

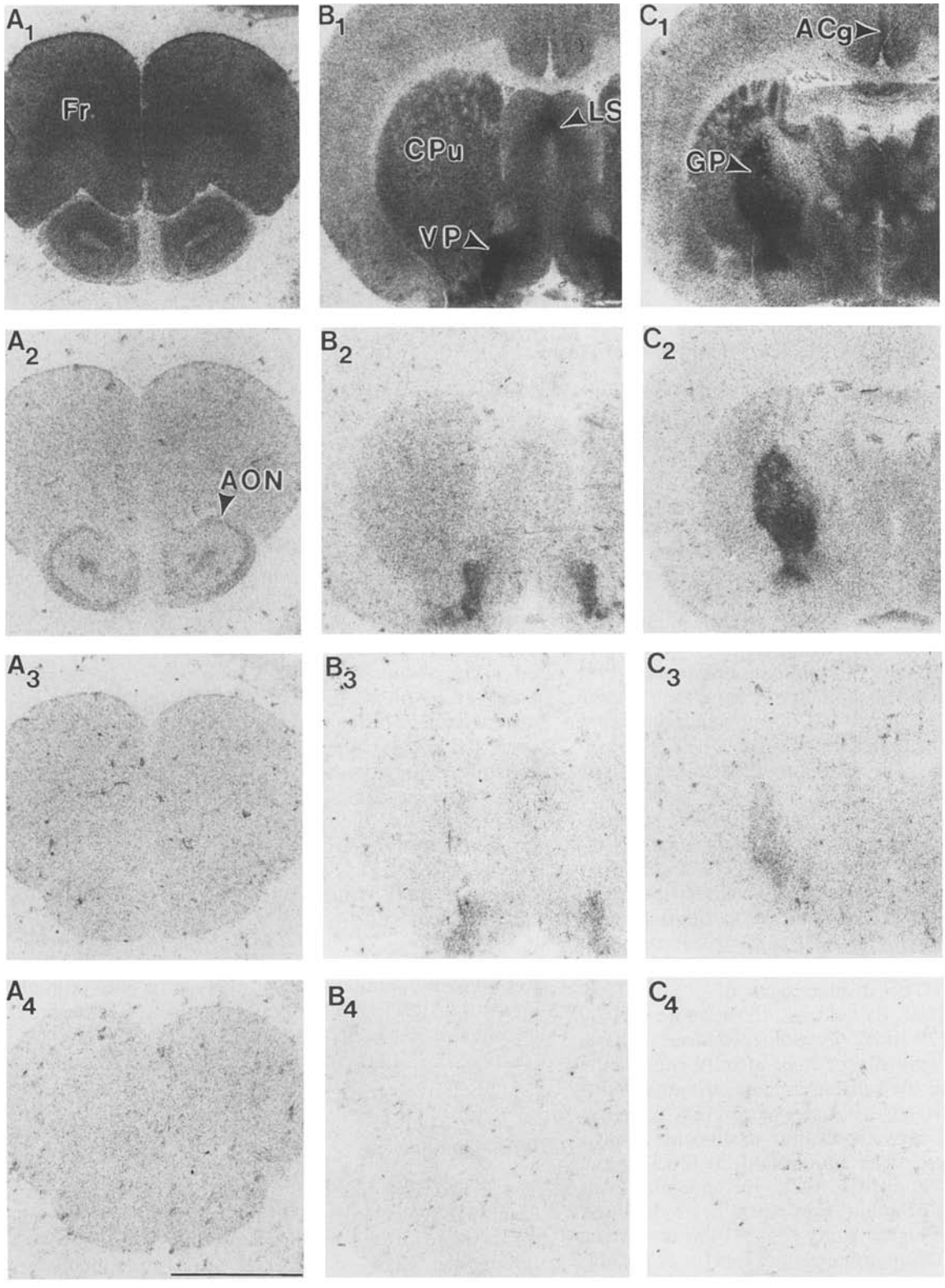

5-HT_1 (5-HT_{1A-1F}) receptor subtypes have been cloned (for reviews see Hartig 1989; Hartig et al. 1992 and McAllister et al. 1992; Levy et al. 1992; Amlaiky et al. 1992).

The 5-HT_{1B} and 5-HT_{1D} receptor subtypes were considered as those [^{3}H]5-HT binding sites showing low affinity for 5-HT_{1A} and 5-HT_{1C} receptor ligands. Due to very distinct pharmacological profiles, the subtype found in rodents (rat, mouse, opossum and hamster) was named 5-HT_{1B} (Hoyer et al. 1985; Waeber et al. 1989a; Waeber and Palacios 1992) whereas in species such as man, pig, guinea-pig, calf, pigeon, dog, rabbit and monkey the 5-HT_{1D} site was described (Heuring and Peroutka 1987; Waeber et al. 1988; Waeber et al. 1989a, 1989b; Bruinvels et al. 1992; Hoyer et al. 1992). The pharmacological differences between the 5-HT_{1B} and 5-HT_{1D} receptor sub-

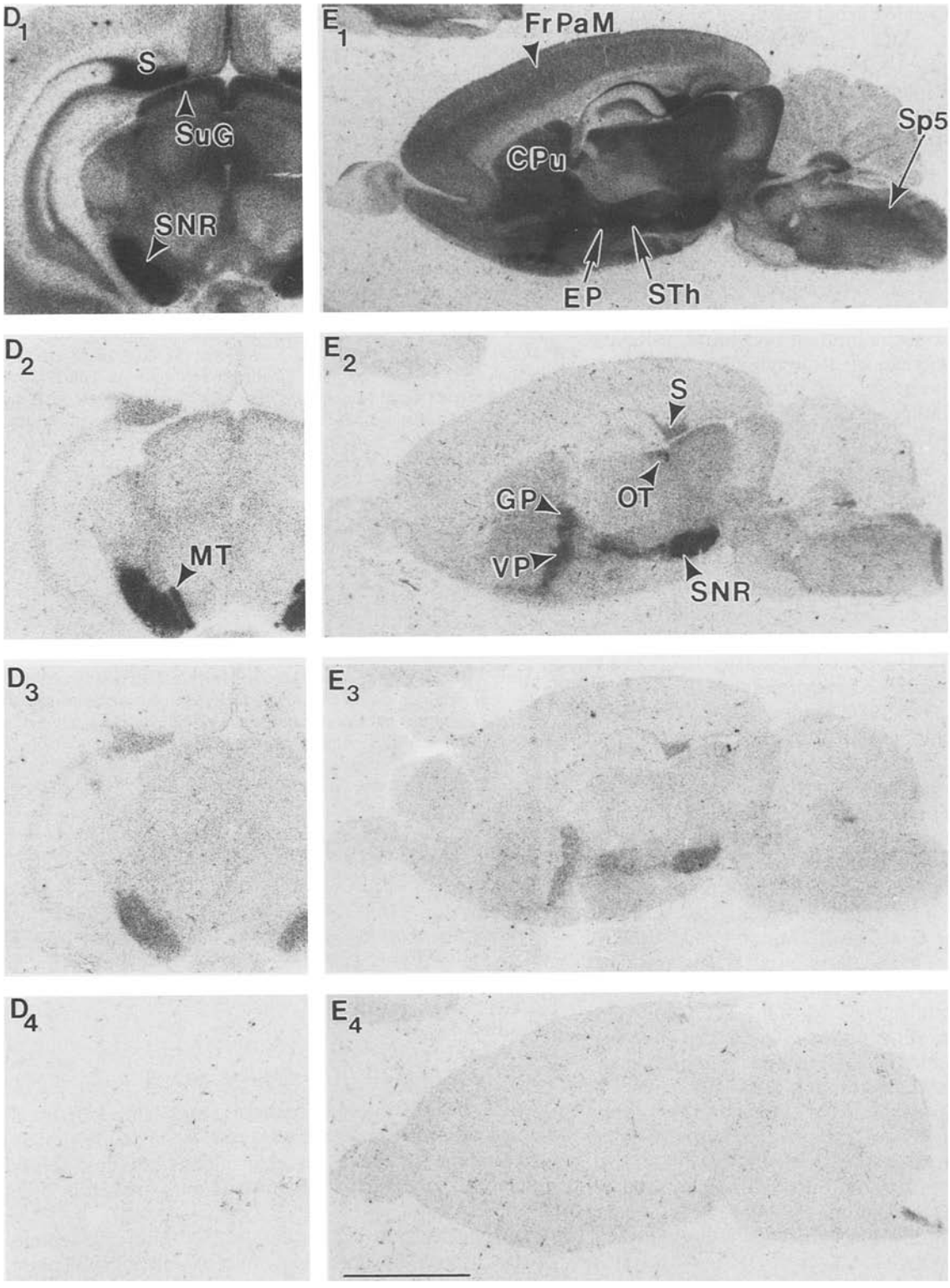

Fig. 1. Photographs of autoradiograms of coronal (**A–D**) and sagittal (**E**) sections labelled with [^{125}I]GTI as described in material and methods. Depicted are the levels of the frontal cortex (**A**), the forebrain (**B**), the basal ganglia (**C**), the midbrain (**D**). A_1-E_1 shows total [^{125}I]GTI binding; $\mathbf{A_2}-\mathbf{E_2}$: [^{125}I]GTI binding performed in the presence of 100 nM CP 93129 (representing virtually all non 5-HT_{1B} binding sites); $\mathbf{A_3}-\mathbf{E_3}$: [^{125}I]GTI binding sites in the presence of 100 nM CP 93129 and 100 nM PAPP (non 5-$HT_{1B/1D}$ binding); $\mathbf{A_4}-\mathbf{E_4}$: non-specific binding (defined in the presence of 10 mM 5-HT). Note the amounts of non 5-HT_{1B} binding displaced by PAPP in the anterior olfactory nucleus (*AON*, $\mathbf{A_{2-3}}$), the caudate-putamen (*CPu*, $\mathbf{B_{2-3}}$), the globus pallidus (*GP*, $\mathbf{C_{2-3}}$), the substantia nigra (reticular part, *SNR*) and the medial nucleus of the accessory optic tract (*MT*, $\mathbf{D_{2-3}}$). To be noticed in pictures $\mathbf{D_{2-3}}$, the minimal displacement of [^{125}I]GTI binding by PAPP in the dorsal subiculum (*S*), suggesting the absence of 5-HT_{1D} sites in this region. *ACg*, anterior cingulate cortex; *EP*, entopeduncular nucleus; *Fr*, frontal cortex; *FrPaM*, frontoparietal cortex, motor area; *LS*, lateral septal nucleus; *Sp5*, spinal nucleus of the trigeminal nerve; *STh*, subthalamic nucleus; *SuG*, superficial gray layer of the superior colliculus; *VP*, ventral pallidum. *Scale bar* = 5 mm

types were clearly revealed using radioligand binding and functional studies. The β-adrenoceptor antagonists (−)iodocyanopindolol (ICYP), (−)pindolol and (−)propranolol show much higher affinities for 5-HT_{1B} sites than for 5-HT_{1D} recognition sites, whereas the α_2-adrenoceptor antagonists rauwolscine and yohimbine have higher affinity for 5-HT_{1D} binding sites. Further, the arylpiperazine PAPP (4[2-[4-[3-(trifluoromethyl)phenyl]-1-piperazinyl]ethyl]benzeneamine) was shown to be selective for 5-HT_{1D} versus 5-HT_{1B} sites (Schoeffter and Hoyer 1989), while the newly synthesised compound CP 93129 (5-methoxy-3-[1,2,3,6-tetra-hydropyridin-4-yl]1-H-indole) has clearcut 5-HT_{1B} selectivity (Macor et al. 1990). Visualisation of the binding sites in rat, using e.g. [^{125}I]ICYP (in presence of isoprenaline to eliminate binding to β-adrenoceptors), and human brain (using e.g. [^{3}H]5-HT as a radioligand and 100 nM 8-hydroxy-[2N-dipropylamino]tetralin (8-OH-DPAT) and mesulergine in order to saturate 5-HT_{1A} and 5-HT_{1C} sites, respectively) revealed the same typical distribution for both receptor subtypes, i.e. high densities of binding sites in substantia nigra, globus pallidus and dorsal subiculum (Pazos and Palacios 1985; Waeber et al. 1989a, 1989b; Sijbesma et al. 1991; Palacios et al. 1992; Waeber and Palacios 1992). Additionally 5-HT_{1B} and 5-HT_{1D} receptor subtypes were found to be both negatively coupled to adenylate cyclase (Bouhelal et al. 1988; Hoyer and Schoeffter 1988) and to represent terminal auto- or heteroreceptors (Engel et al. 1986; Maura and Raiteri 1986; Maura et al. 1986; Middlemiss et al. 1988; Schipper and Tulp 1988; Schlicker et al. 1989; Galzin et al. 1992). Subsequently, it was suggested that the two subtypes represent species variants of the same receptor, thus products of related genes, rather than distinct receptor subtypes (Hoyer and Middlemiss 1989). Finally, the cloning of these genes revealed that, indeed, two very homologous genes code for pharmacologically different receptors in rat and man (Voigt et al. 1991; Jin et al. 1992; Adham et al. 1992; Hamblin et al. 1992a). However, very recent molecular biological work provides evidence that at least two different subtypes of the 5-HT_{1D} receptor, named 5-$HT_{1D\alpha}$ and 5-$HT_{1D\beta}$, are present in human brain, showing virtually identical pharmacology (Hamblin and Metcalf 1991; Hamblin et al. 1992a; Jin et al. 1992; Weinshank et al. 1992). The rat and the mouse equivalents of the human 5-$HT_{1D\beta}$ receptor have been cloned and express the typical 5-HT_{1B} pharmacological profile (Voigt et al. 1991; Adham et al. 1992; Maroteaux et al. 1992). Furthermore, a recent report describes the cloning of the rat 5-$HT_{1D\alpha}$ gene, which shows 5-HT_{1D}-like pharmacology (Hamblin et al. 1992b).

The aim of the present study was to characterise and localise putative 5-HT_{1D} binding sites in rat brain, using in vitro receptor autoradiography, since their existence had been suggested by cloning work. Since [^{125}I]GTI has been introduced as a selective ligand for 5-HT_{1B} and 5-HT_{1D} binding sites in rat and guinea-pig brain, respectively (Boulenguez et al. 1991, 1992), we postulated that this radioligand could detect 5-HT_{1D}, in addition to 5-HT_{1B}, binding sites in rat brain.

Materials and methods

Male Wistar albino rats (250–300 g) were decapitated and the brains quickly removed and placed on dry ice. Tissue sections were cut in 10 µm thick slices with a microtome-cryostat, thaw-mounted onto gelatinised microscope slides and stored at −20 °C until use. The incubations were made according to the following procedure: after two 15 min preincubations in 170 mM Tris-HCl (pH 7.5) containing 4 mM $CaCl_2$, the slides were incubated for 1 h ([^{125}I]GTI) or 2 h ([^{125}I]ICYP) at room temperature in the same medium supplemented with 10 µM pargyline and 0.01% ascorbic acid and 50 pM [^{125}I]GTI or 70 pM [^{125}I]ICYP in the presence or absence of competing drug. Alternate sections to those incubated with [^{125}I]GTI were labelled with [^{125}I] ICYP. Non-specific binding was determined in the presence of 10 µM 5-HT. The washing of labelled sections was carried out as follows: a brief dipping in icecold preincubation buffer followed by two 5-min washes in the same buffer and a brief dipping in distilled water to remove the salts (both icecold). Finally the sections were quickly dried under a stream of cold air. Autoradiograms were generated by apposing the labelled tissues to ^{3}H-Hyperfilms (Amersham, Buckinghamshire, UK) along with Amersham iodinated polymer standards. For [^{125}I]GTI, the films were developed after ten days exposure at 4 °C, while eight hours were sufficient for the [^{125}I]ICYP films. Autoradiograms were quantified with a computerised image-analysis system (MCID, Imaging Research, St. Catherines, Ontario, Canada). Competition curves were generated using non-linear regression analysis using the Grafit package (Erithacus Software Ltd., Staines, UK).

B_{max} values were obtained by correcting the number of receptors bound per milligram of protein (B) for full occupancy of the receptor:

$$B_{max} = B[1+K_D/L]$$

where K_D = affinity constant (derived from literature sources) and L = concentration of radioactive ligand. However, it must be mentioned that this equation represents the binding to a single class of binding sites and the calculated B_{max} value is therefore only an approximation of the maximal number of binding sites of a heterogeneous population. Experiments were performed using three or more rats in at least two experiments.

Drugs. PAPP and 8-OH-DPAT (HBr) were purchased from Research Biochemicals Inc.(Natick, MA, USA). GTI was synthesised by Dr. J. Nozulak (Sandoz Pharma Ltd. Basel, Switzerland) and custom labelled by ANAWA (2175 Ci/mmol, Wangen, Switzerland). [^{125}I]ICYP (2175 Ci/mmol) was obtained from Amersham (Buckinghamshire, UK). CP 93129 was donated by Pfizer (Groton, CT, USA) and all other compounds were synthesised at Sandoz Pharma Ltd. (Basel, Switzerland).

Results

Distribution of [^{125}I]GTI binding sites in rat brain

As can be seen in Fig. 1 (panels 1) and Table 1 (first column) very high amounts ($B_{max} \geqslant 2500$ fmol/mg protein) of binding sites were found in globus pallidus, ventral pallidum, entopeduncular nucleus and substantia nigra (reticular part).

High densities ($1200 \leqslant B_{max} \leqslant 2500$ fmol/mg protein) were observed in subthalamic nucleus, dorsal subiculum, dorsal hypothalamic area, ventral medial hypothalamic nucleus, olivary pretectal nucleus, superficial gray layer of the superior colliculus, central gray and substantia nigra (compact part, Table 1 and Fig. 1).

Intermediate levels ($400 \leqslant B_{max} \leqslant 1200$) of [^{125}I]GTI binding sites were found in many structures of the rat brain, such as olfactory tubercle, anterior olfactory nucleus, nucleus accumbens, nucleus of the optic tract, geniculate nuclei, amygdaloid nuclei, later septal nucleus, opti-

Table 1. Maximal densities of [^{125}I]GTI and [^{125}I]ICYP binding and percentages of [^{125}I]GTI binding displaced by 5-HT$_{1D}$ selective compounds:

AREA	Radioligand			
	[^{125}I]GTI			[^{125}I]CYP
	$B_{max} \pm$ SEM (fmol/mg protein)	% binding displaced by 100 nM PAPP	% binding displaced by 1 μM 8-OH-DPAT	$B_{max} \pm$ SEM (fmol/mg protein)
Olfactory system				
Primary olfactory cortex	283.2± 30.3	15.7±2.6	10.4±2.4	385.0± 25.2
Olfactory tubercle	646.3± 57.1	20.5±4.5	10.9±4.2	518.3±119.0
Anterior olfactory nucleus	460.1±132.0	26.7±1.6	20.2±6.7	206.0± 18.0
Olfactory tract	83.1± 20.5	24.0±2.7	ND	ND
Amygdala				
Amygdalohippocampal area	607.3± 49.1	≤5	12.8±7.8	451.5± 58.7
Posteromedial cortical amygdaloid nucleus	414.7± 33.0	≤5	≤5	312.9± 57.1
Central amygdaloid nucleus	952.9± 57.8	9.5±3.7	9.5±4.4	441.0± 6.9
Medial amygdaloid nucleus	546.3±196.6	7.2±2.7	12.6±2.0	381.5± 20.4
Lateral amygdaloid nucleus	690.1± 7.7	6.0±2.4	6.5±2.8	375.5± 9.0
Basolateral amygdaloid nucleus	623.8± 55.8	5.8±2.5	8.4±5.3	419.6± 16.8
Septal region				
Lateral septal nucleus, intermediate part	819.8±205.3	≤5	≤5	582.7± 76.6
Lateral septal nucleus, ventral part	538.8± 32.7	6.9±3.1	6.2±2.3	280.5± 11.5
Septohippocampal nucleus	906.2±287.2	8.1±3.2	8.7±2.6	763.7± 42.6
Stria terminalis	526.0± 25.7	9.1±0.6	6.2±1.9	271.0± 30.1
Bed nucleus of the stria terminalis	521.7± 41.3	ND	ND	328.9± 23.6
Bed nucleus of the stria terminalis, preoptic part	1169.7±185.4	≤5	≤5	534.2± 85.2
Anterior commissure	132.9± 34.7	30.0±7.0	ND	ND
Basal ganglia				
Accumbens nucleus	1015.4±104.7	10.9±1.8	8.5±1.9	697.0± 44.2
Globus pallidus	3099.0±446.0	17.0±7.3	19.1±8.7	795.0± 14.0
Ventral pallidum	3152.8±467.9	9.6±0.3	7.2±0.6	779.8± 19.0
Entopeduncular nucleus	3190.3±424.0	10.8±4.3	13.3±6.3	683.0±166.0
Caudate-putamen	559.9± 51.6	11.7±1.8	9.7±1.8	450.6± 40.8
Subthalamic nucleus	1449.8±233.5	14.5±1.7	13.5±2.3	668.8± 33.5
Hippocampus				
Dentate gyrus	226.0± 13.1	ND	ND	207.9± 32.7
CA3 field, oriens layer	416.9± 47.3	6.4±2.5	≤5	367.9± 33.9
Dorsal subiculum	1986.4±357.1	≤5	≤5	742.8± 51.3
Hypothalamus				
Anterior hypothalamic area	1095.8±194.7	≤5	≤5	647.7± 69.7
Dorsal hypothalamic area	1270.1±208.2	ND	ND	713.7± 96.0
Dorsal medial hypothalamic area	934.1±184.5	ND	ND	734.0± 1.0
Lateral hypothalamic area	999.0±144.7	≤5	≤5	634.4± 34.4
Medial mammillary nucleus, medial part	692.8± 76.9	≤5	≤5	606.4± 56.3
Supramammillary nucleus	716.8± 82.0	≤5	≤5	703.0± 59.5
Ventral medial hypothalamic nucleus	1276.2±163.2	6.0±3.1	9.1±3.6	557.0±185.0
Thalamus				
Lateral habenular nucleus	659.5± 80.8	≤5	≤5	579.3±108.0
Medial habenular nucleus	558.9± 46.5	ND	ND	531.0± 24.0
Paraventricular thalamic nucleus	531.3± 72.0	ND	ND	617.7± 27.8
Paraventricular thalamic nucleus, anterior part	556.9± 97.0	≤5	≤5	338.5± 11.0
Venteroposterior thalamic nucleus, medial and lateral parts	161.4± 22.5	14.2±1.0	13.5±3.2	152.0± 12.3
Lateral posterior thalamic nucleus	570.2± 35.4	8.3±2.2	6.2±3.7	416.0± 68.6
Laterodorsal thalamic nucleus	643.7± 81.0	7.2±3.4	12.1±8.9	380.3± 80.8
Anterodorsal thalamic nucleus	449.5± 58.2	11.6±2.1	9.3±3.1	191.0± 3.4
Anteroventral thalamic nucleus	242.5± 38.9	≤5	≤5	342.8± 71.6
Central medial thalamic nucleus	624.1± 33.2	10.8±6.7	8.8±1.6	481.3± 95.2
Mediodorsal thalamic nucleus	422.8± 63.9	ND	ND	605.7±123.0
Parafascicular thalamic nucleus	815.2±120.8	≤5	≤5	363.0±126.8
Paratenial thalamic nucleus	440.4± 34.7	≤5	≤5	511.6±110.5
Reuniens thalamic nucleus	689.9± 82.0	10.3±3.8	11.0±8.6	352.3± 85.1
Visual system				
Nucleus of the optic tract	1127.5±103.2	14.5±2.3	18.7±5.7	596.6± 58.1
Olivary pretectal nucleus	1709.6±348.4	8.1±3.2	10.0±4.1	719.0± 64.4
Medial terminal nucleus of the accessory optic tract	504.0± 53.3	28.3±2.3	ND	ND
Anterior pretectal area	818.9± 69.2	8.8±2.1	6.3±2.9	391.0± 49.3

Table 1 (continued)

AREA	Radioligand			
	[^{125}I]GTI			[^{125}I]CYP
	B_{max} ± SEM (fmol/mg protein)	% binding displaced by 100 nM PAPP	% binding displaced by 1 μM 8-OH-DPAT	B_{max} ± SEM (fmol/mg protein)
Ventral lateral geniculate nucleus, magnocellular part	960.6 ± 170.7	11.7 ± 1.8	14.7 ± 3.1	379.5 ± 22.5
Ventral lateral geniculate nucleus, parvocellular part	656.8 ± 111.2	8.1 ± 1.4	ND	286.5 ± 36.5
Dorsal lateral geniculate nucleus	855.6 ± 84.0	7.6 ± 0.8	8.2 ± 1.2	547.1 ± 48.3
Superficial gray layer of the superior colliculus	1377.8 ± 168.2	5.6 ± 1.1	≤5	630.1 ± 38.9
Optic nerve layer of the superior colliculus	989.5 ± 91.1	≤5	≤5	410.1 ± 10.8
Intermediate gray layer of the superior colliculus	943.9 ± 116.0	5.3 ± 0.6	≤5	402.8 ± 4.4
Supraoptic decussation	107.5 ± 31.9	25.1 ± 1.9	ND	ND
Midbrain				
Central gray	1291.6 ± 96.4	≤5	≤5	649.2 ± 39.3
Substantia nigra, reticular part	4417.1 ± 469.3	10.7 ± 2.7	5.8 ± 1.2	815.2 ± 19.7
Substantia nigra, compact part	1779.0 ± 324.7	7.1 ± 2.1	≤5	527.5 ± 26.3
Interpeduncular nucleus	976.6 ± 251.4	≤5	≤5	760.7 ± 11.1
Ventral tegmental area	1097.2 ± 154.9	6.4 ± 2.8	ND	533.3 ± 60.5
Dorsal raphé nucleus	678.0 ± 39.1	≤5	≤5	489.0 ± 35.2
Red nucleus	612.9 ± 99.8	6.7 ± 3.8	8.5 ± 3.1	342.6 ± 59.8
Zona incerta	931.1 ± 83.3	8.8 ± 2.3	5.6 ± 2.1	566.3 ± 59.8
Claustrum, neo, cingulate, temporal and entorhinal cortex				
Claustrum	434.7 ± 39.9	7.3 ± 1.9	≤5	503.7 ± 55.1
Frontal cortex	319.2 ± 69.5	≤5	≤5	405.7 ± 109.5
Frontal parietal cortex, motor area	207.7 ± 14.4	76 ± 2.7	6.6 ± 4.0	193.5 ± 21.5
Frontal parietal cortex, somatosensory area	224.8 ± 13.9	8.1 ± 1.9	7.6 ± 2.7	226.2 ± 27.0
Striate cortex, area 17	231.7 ± 60.7	≤5	≤5	145.7 ± 84.1
Striate cortex, area 18	230.5 ± 58.2	≤5	≤5	127.4 ± 45.0
Striate cortex, area 18a	265.0 ± 32.7	≤5	≤5	184.0 ± 26.0
Anterior cingulate cortex	540.0 ± 90.8	6.5 ± 2.2	≤5	468.8 ± 27.5
Posterior cingulate cortex	900.6 ± 68.4	≤5	≤5	ND
Retrosplenial cortex	638.4 ± 67.0	≤5	≤5	492.5 ± 75.1
Temporal cortex, auditory area	455.4 ± 64.8	≤5	≤5	311.2 ± 69.9
Entorhinal cortex	592.6 ± 36.7	≤5	≤5	421.8 ± 33.4
Medulla oblongata and pons				
Central nucleus of the inferior colliculus, ventral part	653.5 ± 3.9	≤5	≤5	344.0 ± 54.7
Nucleus of the spinal tract of the trigeminal nerve, oral part	424.6 ± 133.3	20.1 ± 5.3	16.1 ± 3.6	526.0 ± 29.6
Dorsal parabrachial nucleus	346.2 ± 9.7	9.5 ± 3.9	≤5	387.5 ± 3.5
Ventral parabrachial nucleus	734.2 ± 234.9	10.1 ± 7.1	7.9 ± 4.3	ND
Laterodorsal tegmental nucleus	627.6 ± 245.6	13.0 ± 5.6	11.1 ± 3.9	432.6 ± 56.8
Hypoglossal nucleus	529.7 ± 4.4	ND	ND	766.0 ± 98.2
Facial nucleus	295.3 ± 27.7	7.8 ± 5.1	7.6 ± 2.2	ND
Cuneiform nucleus	678.8 ± 251.2	6.8 ± 0.9	7.9 ± 3.5	ND
Inferior olive	394.0 ± 35.5	ND	ND	ND
Medial vestibular nucleus	457.9 ± 25.3	ND	ND	703.1 ± 13.5
Cerebellum				
Lateral cervical nucleus	474.1 ± 44.7	≤5	≤5	451.0 ± 23.6
Interpositus cerebellar nucleus	365.2 ± 76.9	≤5	7.0 ± 4.8	452.6 ± 32.9
Choroid plexus				
Third, fourth and lateral ventricle	158.0 ± 30.7	14.9 ± 0.8	15.4 ± 2.3	34.0 ± 17.2

ND = not determined

cal and intermediate gray layer of the superior colliculus, anterior pretectal area, medial terminal nucleus of the accessory optic tract, dorsal raphé nucleus, interpeduncular nucleus and ventral tegmental area; a complete list is to be found in Table 1.

Low densities ($B_{max} \leqslant 400$ fmol/mg protein) of binding sites were observed in different cortical areas, such as primary olfactory cortex, frontal cortex, frontoparietal cortex and striate cortex (for complete list see Table 1).

Pharmacology of [^{125}I]GTI binding sites in rat brain

To determine whether the binding sites labelled with [^{125}I]GTI were heterogeneous, [^{125}I]GTI binding was displaced using the following compounds: 5-CT, CP 93129, sumatriptan, (−)pindolol, rauwolscine and PAPP. Competition curves were generated for the following regions of the rat brain: substantia nigra (reticular part), globus pallidus, caudate-putamen, ventral lateral geniculate nu-

cleus (magnocellular part), nucleus of the optic tract, superficial gray layer of the superior colliculus, central gray and dorsal subiculum of the hippocampus (see Fig. 2). The displacement by 5-CT was monophasic in all structures of the rat brain studied (Fig. 2). By contrast, the drugs CP 93129, (−)pindolol, PAPP and sumatriptan displaced the specific binding in a biphasic manner (Fig. 2). The proportion of high and low affinity sites were compared for the different 5-HT_{1B} compounds ((−)pindolol and CP 93129) and were found to be generally similar, approximately 80% high affinity sites and 20% low affinity sites in the various regions studied (Table 2). For the 5-HT_{1D} selective drug (PAPP) the 'inverse' proportions were observed, thus a minority of high affinity sites and a majority of low affinity sites. Since the selectivity of sumatriptan for both sites (only about ten-fold) is too limited, the proportions detected using sumatriptan do not per se correspond to those found with PAPP (see discussion). Note also the different percentages of high and low affinity sites in the ventral lateral geniculate nucleus (magnocellular part) and the nucleus of the optic tract, which are very small structures and therefore liable to variability. To characterise the minor non 5-HT_{1B} component of the [^{125}I]GTI binding, 5-HT_{1B} recognition sites were blocked with 100 nM CP 93129 and the remaining binding was displaced with low concentrations of PAPP, rauwolscine and 8-OH-DPAT (see Fig. 3). It can be noticed that not all [^{125}I]GTI binding (measured in the presence of 100 nM CP 93129) is displaced by the 5-HT_{1D} compounds; this suggests that 100 nM CP 93129 did not block all 5-HT_{1B} binding. The averaged pK_D values (determined in various brain structures) were ordered for the major and the minor components of [^{125}I]GTI binding and are listed in Table 3. The rank order of affinity of the major component corresponds to that of a 5-HT_{1B} site (determined in rat cortex homogenates using [^{125}I]ICYP as a radioligand (Hoyer et al. 1985, $r = 0.97$), whereas that of the minor component matches a 5-HT_{1D} binding profile (determined in human substantia nigra homogenates with [^{125}I]GTI (Bruinvels et al. 1991, $r = 0.96$), as shown in Fig. 4.

Distribution of 5-HT_{1D} binding sites in rat brain

By masking the majority of the 5-HT_{1B} recognition sites with 100 nM CP 93129, the putative 5-HT_{1D} binding sites were visualised. The remaining binding was as expected displaced with PAPP (Fig. 1, panels 2–3) or 8-OH-DPAT. Thus, as can be seen in Fig. 1, the 5-HT_{1D} sites are represented as the difference between panel 2 and 3. The remaining sites shown in panel 3 correspond to the low affinity component pictured in Fig. 3 (see above). The densities of 5-HT_{1D} sites were estimated by displacing the non 5-HT_{1B} [^{125}I]GTI binding sites with 100 nM PAPP or 1 μM 8-OH-DPAT (Table 1). In general, the percentages displaced with both compounds were very comparable. For further discussion of these PAPP and 8-OH-DPAT sensitive [^{125}I]GTI binding sites, only considered were structures in which more than 5% of total [^{125}I]GTI binding was displaced by the two compounds. Low densities of PAPP/8-OH-DPAT sensitive [^{125}I]GTI binding sites (expressed in percentage of total [^{125}I]GTI binding sites) were localised throughout the rat brain and represented a minor component of [^{125}I]GTI binding sites (Table 1, Fig. 1). Hence, no region was found to display the presence of solely 5-HT_{1D} binding sites. Relative to the total amount of specific binding (expressed in fmol/mg protein) observed in the different regions, the highest levels were found in primary olfactory cortex, central and medial amygdaloid nuclei, globus pallidus, entopeduncular nucleus, ventral pallidum and substantia nigra (reticular part) and in some regions of the brainstem (Table 1, Fig. 1). 5-HT_{1D} binding sites were also present in some thalamic nuclei and very clearly in medial terminal nucleus of the accessory optic tract, nucleus of the optic tract and ventral lateral geniculate nucleus. Noticeably, many fiber tracts, such as supraoptic decussation, olfactory tract, stria terminalis and anterior com-

Table 2. Affinity values (pK_D, −log mol/l) of different drugs for high and low affinity [^{125}I]GTI binding sites (percentage of specific binding) in different structures of the rat brain

Area	(−)Pindolol				CP 93129				Sumatriptan				PAPP			
	High	pK_D	Low	pK_D	High	pK_D	Low	pK_D	High	pK_D	Low	pK_D	High	pK_D	Low	pK_D
SNR	82%	8.52	18%	5.96	77%	7.92	23%	5.76	51%	7.83	49%	6.69	38%	7.80	62%	6.12
GP	75%	8.09	25%	7.15	70%	8.64	30%	6.34	22%	8.54	78%	6.97	27%	8.49	73%	6.37
VP	70%	7.92	30%	5.84	65%	8.84	35%	6.23	60%	7.82	40%	6.65	41%	8.44	59%	6.42
CPu	81%	8.07	19%	6.03	65%	8.63	35%	6.05	74%	7.63	26%	6.27	31%	7.64	69%	6.34
VLGMC	38%	8.60	62%	7.10	89%	8.16	11%	6.43	33%	7.97	67%	7.11	38%	7.68	62%	6.27
OT	39%	8.35	61%	6.87	74%	8.25	26%	6.08	70%	7.92	30%	6.73	28%	8.60	72%	6.54
SuG	86%	8.13	14%	5.75	71%	8.40	29%	7.02	60%	7.74	40%	6.12	27%	8.11	73%	6.60
MT	67%	8.05	33%	5.87	76%	7.96	24%	5.50	ND	ND	ND	ND	ND	ND	ND	ND
CG	92%	8.10	8%	6.38	83%	8.23	17%	6.44	54%	8.15	46%	7.01	14%	8.68	86%	6.69
S	100%	7.96			100%	7.39					100%	7.13			100%	6.48
Mean pK_D	8.18 ± 0.07		6.33 ± 0.19		8.24 ± 0.13		6.21 ± 0.15		7.95 ± 0.10		6.74 ± 0.12		8.02 ± 0.24		6.43 ± 0.06	

Abbreviations used: CG, central (periaqueductal) gray; CPu, caudate putamen; GP, globus pallidus; MT, medial terminal nucleus of the accessory of optic tract; OT, nucleus of the optic tract; S, subiculum; SNR, substantia nigra, reticular part; SuG, superficial gray layer of the superior colliculus; VLGMC, ventral lateral geniculate nucleus, magnocellular part; VP, ventral pallidum; ND, not determined

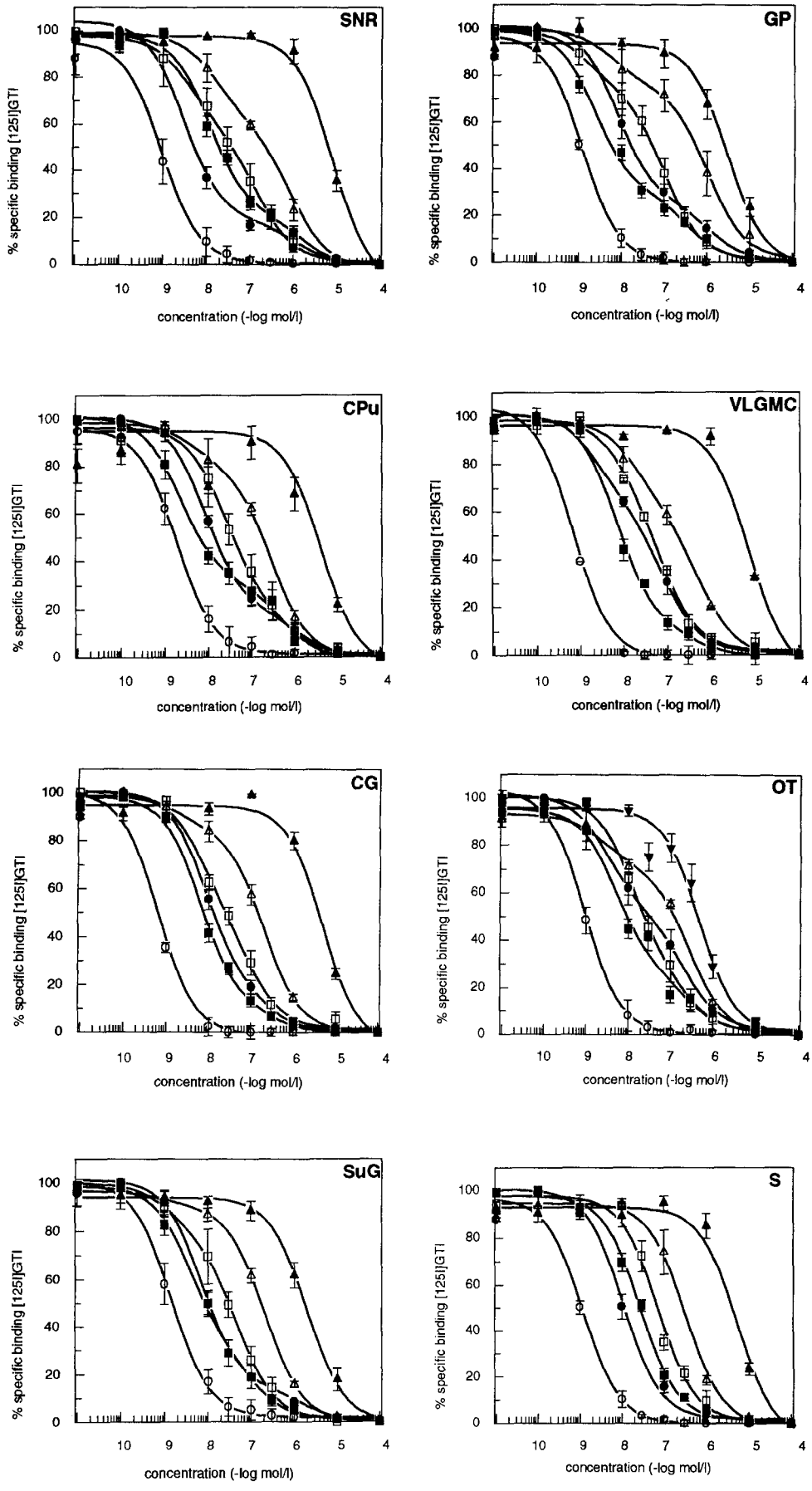

Fig. 2. Competition curves generated using quantitative autoradiography as described in Material and methods. Specific [^{125}I]GTI binding was displaced by 6 or 8 concentrations of drugs. Curves correspond to (○) 5-CT, (■) CP 93129, (●) (−)pindolol, (□) sumatriptan, (△) PAPP, (▲) rauwolscine or (▼) yohimbine. *CG*, central (periaqueductal) gray; *CPu*, caudate putamen; *GP*, globus pallidus; *OT*, nucleus of the optic tract; *S*, subiculum; *SNR*, substantia nigra, reticular part; *SuG*, superficial gray layer of the superior colliculus; *VLGMC*, ventral lateral geniculate nucleus, magnocellular part

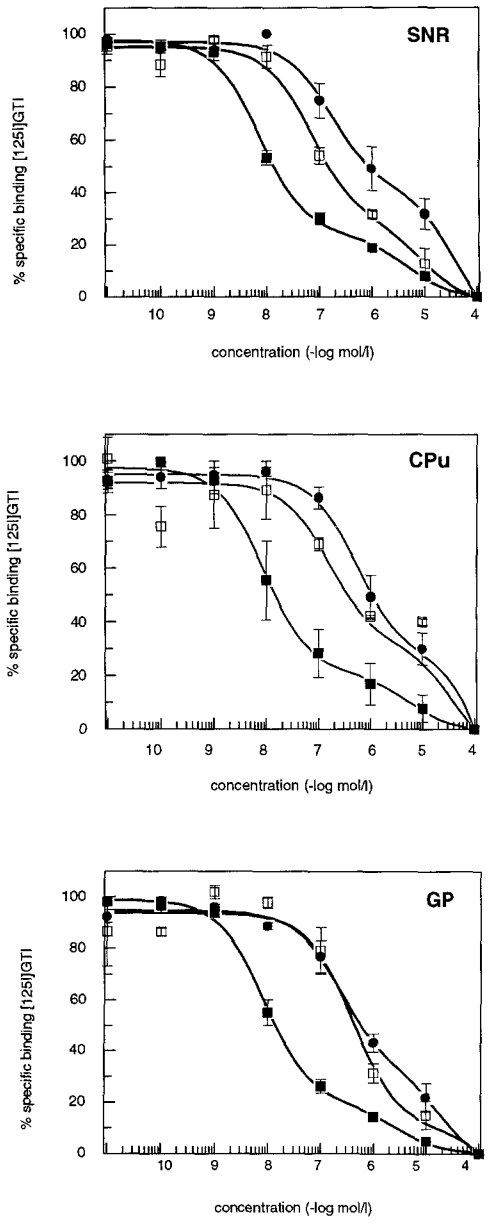

Fig. 3. Competition curves of [^{125}I]GTI binding (carried out in the presence of 100 nM CP 93129) by PAPP (■), rauwolscine (□) and 8-OH-DPAT (●) in the reticular part of the substantia nigra (*SNR*), caudate-putamen (*CPu*) and globus pallidus (*GP*). Note that the high affinity component of the displacement curves corresponds to 5-HT$_{1D}$ sites, whereas the low affinity component represents probably remaining 5-HT$_{1B}$ binding sites (not blocked by 100 nM CP 93129)

missure, showed specific 5-HT$_{1D}$ binding (Table 1, Fig. 1).

Comparison of [^{125}I]ICYP and [^{125}I]GTI binding sites

To verify whether [^{125}I]GTI labels a larger population of binding sites than the 5-HT$_{1B}$ radioligand [^{125}I]ICYP, alternate sections to those labelled with [^{125}I]GTI were incubated with [^{125}I]ICYP (in the presence of 100 nM 8-OH-DPAT and 3 μM isoprenaline to mask 5-HT$_{1A}$ binding sites and β-adrenoceptors). The distributions of sites labelled with either radioligand were very similar as illustrated in Fig. 5. Qualitative comparison of the distribution of recognition sites reveals less [^{125}I]ICYP labelling in several structures, such as medial terminal nucleus of the accessory optic tract, anterior parts of the thalamus and the caudate-putamen (Fig. 5). Further, clearcut differences of the B_{max} values of [^{125}I]ICYP and [^{125}I]GTI binding can be observed in different structures of the rat brain (Table 1). As listed in Table 1, the maximal densities of binding sites for the two radioligands can be roughly compared in regions of intermediate labelling. However, in structures where high or very high densities

Table 3. Affinity values (pK_D, −log mol/l) for 5-HT$_{1D}$ (minor component of [^{125}I]GTI binding) and 5-HT$_{1B}$ (major component of [^{125}I]GTI binding) sites in rat brain obtained with receptor autoradiography. The data represent mean pK_D values determined in the brain areas listed in Table 2

Drug	5-HT$_{1D}$	5-HT$_{1B}$
5-CT	9.13 ± 0.06	9.13 ± 0.06
PAPP	8.02 ± 0.24	6.43 ± 0.06
Sumatriptan	7.95 ± 0.10	6.74 ± 0.12
Rauwolscine	7.15 ± 0.06[a]	5.11 ± 0.09
8-OH-DPAT	6.88 ± 0.06[a]	4.45 ± 0.21
(−)Pindolol	6.33 ± 0.19	8.18 ± 0.07
CP 93129	6.21 ± 0.15	8.24 ± 0.13

[a] Affinity values obtained in the presence of 100 nM CP 93129

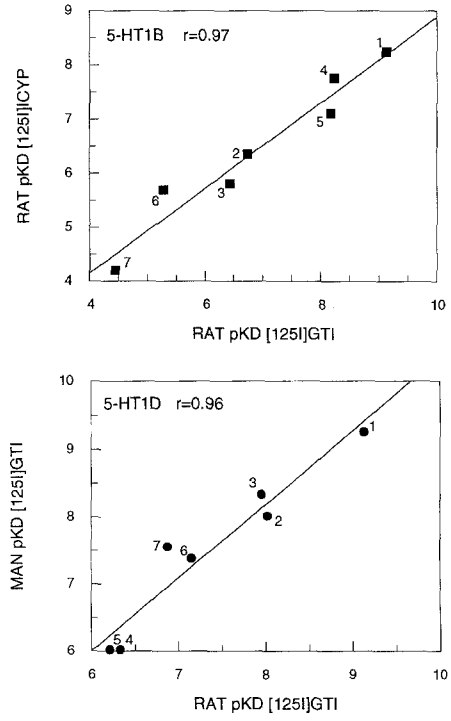

Fig. 4. Correlation of pK$_D$ values of the 5-HT$_{1B}$ and 5-HT$_{1D}$ [^{125}I]GTI binding sites in rat brain (data taken from Table 3) with affinity values measured in rat cortex homogenates using [^{125}I]ICYP (5-HT$_{1B}$ sites, Hoyer et al. 1985) and [^{125}I]GTI binding sites in human substantia nigra homogenates (5-HT$_{1D}$ sites, Bruinvels et al. 1991, except *3* and *6*, where data were obtained in calf caudate using [^{3}H]-5-HT, Waeber et al. 1988), respectively. pK$_D$ values of *4* are unpublished observations (Hoyer). The numbers indicate the following compounds: *1*, 5-CT; *2*, sumatriptan; *3*, PAPP; *4*, CP 93129; *5*, (−)pindolol; *6*, rauwolscine; *7*, 8-OH-DPAT

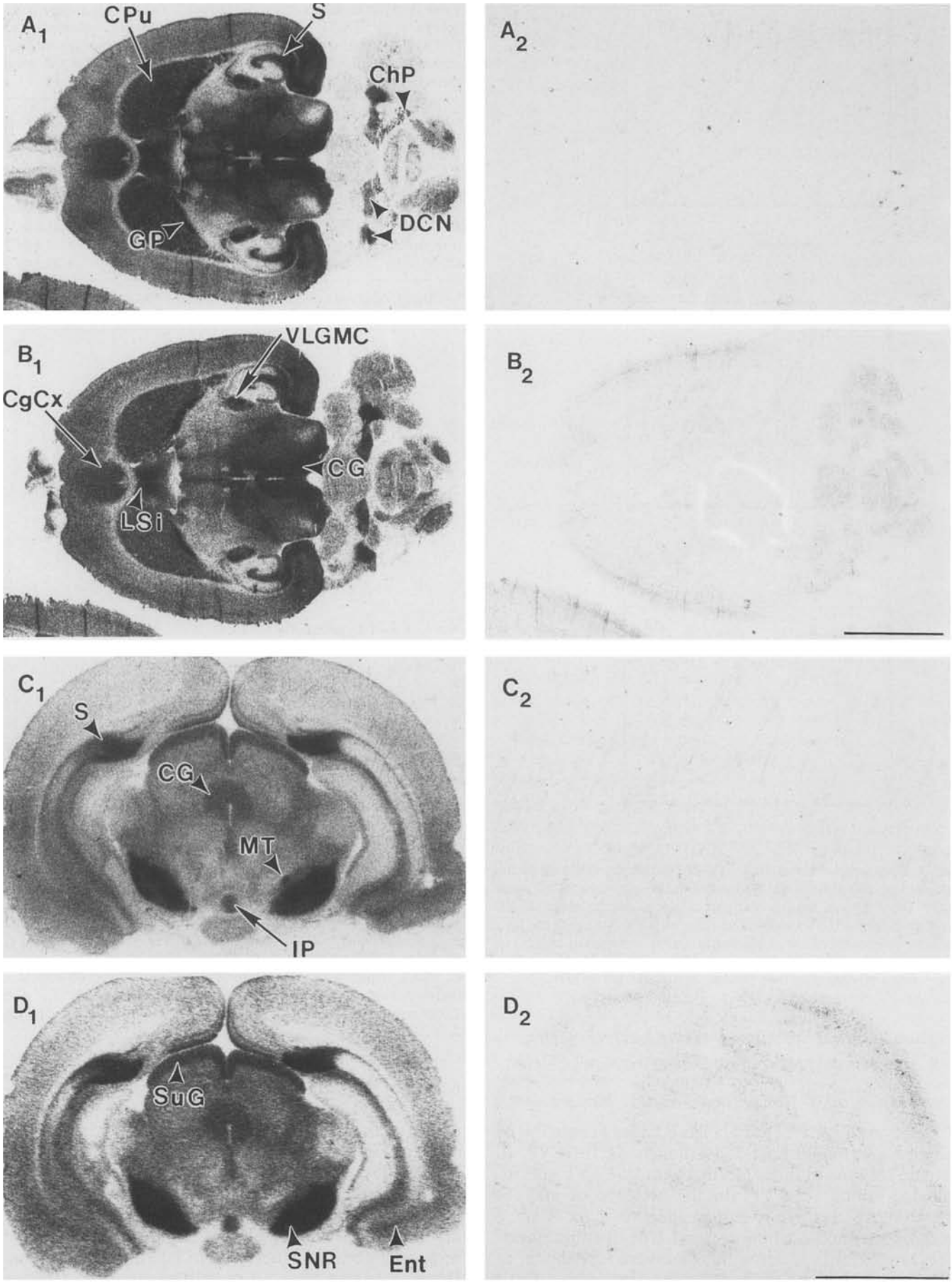
A1
CPu
S
ChP
GP
DCN
A2
B1
VLGMC
CgCx
CG
LSi
B2
C1
S
CG
MT
IP
C2
D1
SuG
SNR
Ent
D2

of binding sites were observed, large variations in the B_{max} values of the two radioligands were found: e.g. the difference of [^{125}I]GTI binding observed in substantia nigra versus subiculum is twofold in contrast to more or less equal amounts of binding when labelled with [^{125}I]ICYP (see Table 1, Fig. 5).

Discussion

The present quantitative of receptor autoradiographic study was performed in order to investigate the possible presence and distribution of 5-HT$_{1D}$ binding sites in rat brain. With the use of the selective 5-HT$_{1B/1D}$ radioligand [^{125}I]GTI, the identification of 5-HT$_{1D}$ binding sites in rat brain was indeed made possible. The pharmacological profile of these 5-HT$_{1D}$ sites was in good agreement with 5-HT$_{1D}$ affinity values reported previously in species lacking 5-HT$_{1B}$ binding (Bruinvels et al. 1991, 1992). 5-HT$_{1D}$ sites were detected in several areas of rat brain, but higher densities of 5-HT$_{1B}$ binding sites were consistently detected in the same brain structures.

When comparing the population of binding sites labelled with either [^{125}I]ICYP or [^{125}I]GTI, the distributions of both binding sites appeared to be very similar (Fig. 5), although, some regions (e.g. medial terminal nucleus of the accessory optic tract) were clearly labelled with [^{125}I]GTI whereas [^{125}I]ICYP binding was apparently poor in these structures (Fig. 5). Quantitative analysis revealed differences in the maximal densities of binding sites of both radioligands: the values found with [^{125}I]GTI were consistently higher (Table 1). Interestingly, a similar autoradiographic study performed in rat brain using [^{3}H]5-HT as a radioligand, revealed that the B_{max} values of sites labelled with [^{125}I]GTI and [^{3}H]5-HT (in the presence of 100 nM 8-OH-DPAT and mesulergine) are in the same order of magnitude (Bruinvels et al. 1993). It has to be mentioned that the B_{max} values were calculated using a single concentration of radioligand, which provides only a rough estimate of the maximal density of binding sites. When only the intermediate dense labelled regions are considered, note e.g. anterior olfactory nucleus, amygdaloid and septal nuclei, dorsal and reuniens thalamic nuclei and various structures of the visual system, comparable B_{max} values are [^{125}I]GTI and [^{215}I]ICYP were detected. However a pharmacological analysis of [^{125}I]GTI labelled sites proved to be a far better method to investigate the possible presence of 5-HT$_{1D}$ sites in rat brain.

The pharmacological analysis of the [^{125}I]GTI binding sites in different areas of rat brain revealed complex displacement of [^{125}I]GTI binding by drugs having distinct affinities for 5-HT$_{1B}$ or 5-HT$_{1D}$ sites. The biphasic curves obtained with (−)pindolol and CP 93129 revealed a major component of high affinity and a minor component of low affinity sites; on the other hand, compounds displaying higher affinity for 5-HT$_{1D}$ than for 5-HT$_{1B}$ sites (PAPP and sumatriptan) produced competition curves with, in general, the inverse proportions (Fig. 2, Table 2). The estimation of the relative proportions of 5-HT$_{1B}$ and 5-HT$_{1D}$ [^{125}I]GTI binding sites by competition experiments, gave the most consistent results with CP 93129 and PAPP, due to their 100-fold selectivity for 5-HT$_{1B}$ or 5-HT$_{1D}$ sites, respectively (Table 2, Fig. 2). Sumatriptan, however, which displays only a ten-fold selectivity for 5-HT$_{1D}$ sites is undoubtedly not selective enough to provide reliable estimates of high/low affinity sites (Table 2). By blocking the 5-HT$_{1B}$ recognition sites with 100 nM CP 93129, the remaining binding sites could be further characterised. The profile of the non 5-HT$_{1B}$ [^{125}I]GTI binding was identified as 5-HT$_{1D}$ (Table 3, Fig. 4). The discrepancy between the monophasic rauwolscine curves displacing total [^{125}I]GTI binding (Fig. 2) and the rauwolscine curves displacing the [^{125}I]GTI binding in the presence of 100 nM CP 93129 (Fig. 3) at low concentrations, remains to be explained. The results show that radioligand binding (using homogenates or whole tissue sections) has clear limitations when it comes to determine the binding profile of a minor (10−20%) binding component with compounds displaying limited selectivity.

Interestingly, [^{125}I]GTI labels a homogeneous population of 5-HT$_{1B}$ binding sites in the dorsal subiculum of the hippocampus (Fig. 2), a region where 5-HT$_{1A}$ and 5-HT$_{1C}$ sites were shown to be absent (Pazos and Palacios 1985). Similar competition curves were obtained using [^{3}H]5-HT, confirming the homogeneity of this rat brain structure (Bruinvels et al. 1993). By contrast, [^{125}I]GTI binding represents a composite of 5-HT$_{1B}$ and 5-HT$_{1D}$ binding sites in most other regions of the rat brain studied (Fig. 2). Clearly, no rat brain region representing a homogeneous population of 5-HT$_{1D}$ binding sites could be identified. The highest proportions of 5-HT$_{1D}$ sites (±30%), labelled with [^{125}I]GTI in rat brain, was found in the medial terminal nucleus of the accessory optic tract and the anterior commissure (Table 1, Fig. 6).

A feature which has not been reported earlier, is the presence of 5-HT$_{1B}$ and 5-HT$_{1D}$ recognition sites in fiber tracts. [^{125}I]GTI binding sites were detected in the olfactory tract, the supraoptic decussation, the stria terminalis and the anterior commissure. Since 5-HT$_{1B}$ and 5-HT$_{1D}$ receptors are presumably located on nerve terminals (and may be transported along the axon), it is possible that these [^{125}I]GTI binding sites represent receptors in transit. In fact, an autoradiographical study has shown that β-adrenoceptors undergoing axonal transport, can exist in a high affinity binding state (Zarbin et al. 1983).

Fig. 5. Photographs of autoradiograms characterising the distribution of [^{125}I]GTI (**A** and **C**) and [^{125}I]ICYP (in presence of 100 nM 8-OH-DPAT and 3 μM isoprenaline, **B** and **D**) binding sites. **A_1−D_1**: total binding; **A_2−D_2**: non-specific binding (defined by 10 μM 5-HT). Note the structures, such as caudate-putamen (*CPu*), which appear to be more densely labelled with [^{125}I]GTI than with [^{125}I]ICYP. *CG*, central (periaqueductal) gray; *CgCx*, cingulate cortex; *ChP*, choroid plexus; *DCN*, deep cerebellar nuclei; *Ent*, entorhinal cortex; *GP*, globus pallidus; *IP*, interpeduncular nucleus; *LSi*, lateral septal nucleus, intermediate part; *MT*, medial terminal nucleus of the accessory optic tract; *S*, subiculum; *SNR*, substantia nigra, reticular part; *SuG*, superficial gray layer of the superior colliculus; *VLGMC*, ventral lateral geniculate nucleus, magnocellular part. *Scale bar* = 5 mm

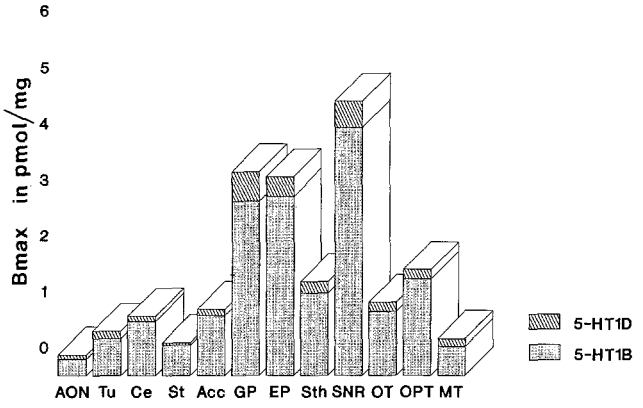

Fig. 6. Bardiagram of maximal densities (pmol/mg protein) of [^{125}I]GTI binding sites and the proportions of 5-HT$_{1D}$ and 5-HT$_{1B}$ sites, in different structures of the rat brain. *Acc*, nucleus accumbens; *AON*, anterior olfactory nucleus; *Ce*, central amygdaloid nucleus; *EP*, entopeduncular nucleus; *GP*, globus pallidus; *MT*, medial terminal nucleus of the accessory optic tract; *OPT*, olivary pretectal nucleus; *OT*, nucleus of the optic tract; *SNR*, substantia nigra, reticular part; *St*, stria terminalis; *STh*, subthalamic nucleus; *Tu*, olfactory tubercle

When first introduced, [^{125}I]GTI was described as being 5-HT$_{1B/1D}$ selective and to label homogeneous populations of binding sites in rat and guinea-pig (Boulenguez et al. 1992). A possible explanation for Boulenguez et al. (1992) not reporting heterogeneity of [^{125}I]GTI binding sites in rat brain, is their choice of drugs in combination with the fact that the Hill coefficient will not deviate notably from unity if the proportion of high/low affinity sites is 80/20. The present data were confirmed in another study (Bruinvels et al. 1993) which describes the heterogeneity of the [^{3}H]5-HT binding sites, remaining after blockade of 5-HT$_{1A}$ and 5-HT$_{1C}$ receptors, in rat brain. Indeed, in brain structures such as substantia nigra and globus pallidus the same biphasic competition curves were observed as with [^{125}I]GTI (Fig. 2), whereas displacement of [^{3}H]5-HT in striatum and cortex was even more complex.

The same type of study as presented here has been performed on human and guinea-pig brain and preliminary results indicate that homogeneous populations of binding sites are labelled with [^{125}I]GTI in human and guinea-pig brain (Bruinvels, Landwehrmeyer, Probst, Palacios and Hoyer, unpublished). [^{125}I]GTI binding in membrane homogenates of human substantia nigra and human caudate was also shown to be homogeneous (Bruinvels et al. 1991, 1992). However, the human homologue of the rat 5-HT$_{1D}$ receptor (5-HT$_{1D\alpha}$), shows a pharmacological profile very similar to that of the 5-HT$_{1D\beta}$ receptor (Hartig et al. 1992; Weinshank et al. 1992); thus, one would not expect to detect heterogeneity of the 5-HT$_{1D}$ receptor subtypes in man with radioligand receptor binding, as we did in rat brain.

The distribution of the 5-HT$_{1D}$ and 5-HT$_{1B}$ sites labelled with [^{125}I]GTI, revealed that both binding sites are expressed in the same structures of the rat brain (Table 1, Figs. 1 and 6). Although no single region expressing exclusively 5-HT$_{1D}$ binding sites was observed, several areas appear to contain 5-HT$_{1B}$ in the absence of 5-HT$_{1D}$ binding sites. Regions expressing both binding sites include globus pallidus, entopeduncular nucleus, subthalamic nucleus, substantia nigra (reticular part), superior colliculus, different subdivisions of the pretectum and structures of the olfactory system. These data suggest that 5-HT$_{1D}$ and 5-HT$_{1B}$ binding sites could both modulate the in- and output of the basal ganglia, an assembly of structures known to be involved in motor functions, the visual and the olfactory system. The cellular localisation of these sites still remains to be investigated, therefore the present data do not allow speculation about pre- or postsynaptic localisation.

Few reports have demonstrated the presence of 5-HT$_{1D}$(-like) binding sites in rat. A radioligand binding study in rat brain homogenates suggested that 5-HT$_{1D}$ binding sites represent 40% of total 5-HT$_1$ sites in hypothalamus, diencephalon, midbrain and brainstem (Herrick-Davis and Titeler 1988). Comparing these results to the present study, these proportions appear to be somewhat overestimated, since hypothalamus and diencephalon showed little non 5-HT$_{1B}$ sites in our study. In addition, although Hamblin et al. (1992b) have cloned the rat 5-HT$_{1D\alpha}$ receptor cDNA, Adham et al. (1992) have been unable to do so. Therefore it seems not very likely that high amounts of 5-HT$_{1D}$ binding sites are present in rat brain. Little has been documented so far to support a functional role for 5-HT$_{1D}$ receptors in rat brain. A behavioural study on hindlimb-scratching in rats suggested the mediation by a possible 5-HT$_{1D}$ receptor subtype, which is probably due to a peripheral mechanism (Berendsen and Broekkamp 1991). A recent study on 5-HT autoreceptors in rabbit, guinea-pig and rat brain, suggested putative 5-HT$_{1D}$-like autoreceptors to be present in rat cortex (Limberger et al. 1991). Although this autoreceptor was not affected by high doses of yohimbine, the effects produced by 8-OH-DPAT (at concentrations known to activate 5-HT$_{1D}$ receptors) were not antagonised by the 5-HT$_{1B}$ receptor antagonist isamoltane (Limberger et al. 1991).

More data have been reported for the 5-HT$_{1B}$ (5-HT$_{1D\beta}$) receptor subtype. Lesion studies in rat striatum have shown that the 5-HT$_{1B}$ binding site in substantia nigra and globus pallidus might be located presynaptically on nerve terminals of striatal projection neurons (Vergé et al. 1986). In situ hybridisation studies, using probes from the rat and mouse 5-HT$_{1B}$ receptor, demonstrate that no mRNA can be detected in globus pallidus, substantia nigra and entopeduncular nucleus, although high hybridisation signals were observed in caudate-putamen and subthalamic nucleus (Voigt et al. 1991; Maroteaux et al. 1992). These data do therefore suggest that the 5-HT$_{1B}$ receptor subtype could be very important as a presynaptic heteroreceptor, regulating the release of different neurotransmitters, such as substance P (Hong et al. 1977) and GABA (Ribak et al. 1980) on projection neurons of the rat basal ganglia. Along similar lines it could be speculated that the 5-HT$_{1D\beta}$ receptor could function similarly in species other than rodents. In addition, it has been shown that 5-HT$_{1B}$ (Engel et al. 1986; Maura et al. 1986; Limberger et al. 1991) and 5-HT$_{1D}$ (Middlemiss et al. 1988; Schipper and Tulp 1988; Galzin et al. 1992; Schlicker et al. 1989; Limberger et al.

1991) autoreceptors can modulate 5-HT release on terminals of neurons ascending from the dorsal and median raphé nucleus projecting to hippocampal structures, striatum and frontal cortex. Thus in rat, 5-HT_{1B} receptors could function as auto- and heteroreceptors, not only in the extrapyramidal system, but also in the hippocampus and probably in the visual system. This is in agreement with the observation that the 5-HT_{1B} mRNA is frequently detected in brain regions from which the neurons originate, whereas the 5-HT_{1B} receptor protein is observed at the putative nerve terminals of these projection neurons (Voigt et al. 1991; Maroteaux et al. 1992). In contrast to this prejunctional location of 5-HT_{1B} receptors, binding sites and mRNA (Voigt et al. 1991) can also be found in the very same structures of the rat brain: subdivisions of the olfactory system, nucleus accumbens, entorhinal cortex, layer IV of the frontal cortex, central gray and subthalamic nucleus are examples of 5-HT_{1B} sites possibly located on cell bodies and/or dendrites, although no functions have been assigned yet.

It still remains to be seen whether the 5-HT_{1D} binding sites, detected in the present study, correspond to the recently cloned 5-$HT_{1D\alpha}$ receptor cDNA. Therefore in situ hybridisation histochemical and lesion studies remain to be carried out in order to elucidate the possible function(s) of these sparsely distributed 5-HT_{1D} binding sites in rat brain.

References

Adham N, Romanienko P, Hartig P, Weinshank RL, Branchek T (1992) The rat 5-hydroxytryptamine$_{1B}$ receptor is the species homologue of the human 5-hydroxytryptamine$_{1D\beta}$ receptor. Mol Pharmacol 41:1–7

Amlaiky N, Ramboz S, Boschert U, Plassat J-L, Hen R (1992) Isolation of a mouse "5-HT1E-like" serotonin receptor expressed predominantly in the hippocampus. J Biol Chem 267:19761–19764

Berendsen HHG, Broekkamp CLE (1991) A peripheral 5-HT_{1D}-like receptor involved in serotonergic induced hindlimb scratching in rats. Eur J Pharmacol 194:201–208

Bouhelal R, Smounya L, Bockaert J (1988) 5-HT_{1B} receptors are negatively coupled with adenylate cyclase in rat substantia nigra. Eur J Pharmacol 151:189–196

Boulenguez P, Chauveau J, Segu L, Morel A, Delaage M, Lanoir J (1991) Pharmacological characterization of serotonin-O-carboxymethyl-glycyl-tyrosinamide, a new selective indolic ligand for 5-hydroxytryptamine (5-HT)$_{1B}$ and 5-HT_{1D} binding sites. J Pharmacol Exp Ther 259:1360–1365

Boulenguez P, Segu L, Chauveau J, Morel A, Lanoir J, Delaage M (1992) Biochemical and pharmacological characterization of serotonin-O-carboxymethylglycyl[^{125}I]iodotyrosinamide, a new radioiodinated probe for 5-HT_{1B} and 5-HT_{1D} binding sites. J Neurochem 58:951–959

Bruinvels AT, Landwehrmeyer B, Waeber C, Palacios JM, Hoyer D (1991) Homogeneous 5-HT_{1D} recognition sites in the human substantia nigra identified with a new iodinated radioligand. Eur J Pharmacol 202:89–91

Bruinvels AT, Lery H, Nozulak J, Palacios JM, Hoyer D (1992) 5-HT_{1D} binding sites in various species: similar pharmacological profile in calf, guinea-pig, dog, monkey and human brain membranes. Naunyn-Schmiedeberg's Arch Pharmacol 346:243–249

Bruinvels AT, Palacios JM, Hoyer D (1993) 5-Hydroxytryptamine$_1$ recognition sites in rat brain: Heterogeneity of non-5-hydroxytryptamine$_{1A/1C}$ binding sites revealed by quantitative receptor autoradiography. Neuroscience 53:465–473

Dumuis A, Bouhelal R, Sebben M, Cory R, Bockaert J (1988) A non-classical 5-hydroxytryptamine receptor positively coupled with adenylate cyclase in the central nervous system. Mol Pharmacol 34:880–887

Engel G, Göthert M, Hoyer D, Schlicker E, Hillenbrand K (1986) Identity of inhibitory presynaptic 5-hydroxytryptamine (5-HT) autoreceptors in the rat brain cortex with 5-HT_{1B} binding sites. Naunyn-Schmiedeberg's Arch Pharmacol 332:1–7

Galzin AM, Poirier MF, Lista A, Chodkiewicz JP, Blier P, Ramdine R, Loo H, Roux FX, Redondo A, Langer SZ (1992) Characterization of the 5-hydroxytryptamine receptor modulating the release of [^{3}H]5-hydroxytryptamine in slices of the human neocortex. J Neurochem 59:1293–1301

Hamblin MW, Metcalf MA (1991) Primary structure and functional characterization of a human 5-HT_{1D}-type serotonin receptor. Mol Pharmacol 40:143–148

Hamblin MW, Metcalf MA, McGuffin RW, Karpells S (1992a) Molecular cloning and functional characterization of a human 5-HT_{1B} serotonin receptor: a homologue of the rat 5-HT_{1B} receptor with a 5-HT_{1D}-like pharmacological specificity. Biochem Biophys Res Commun 184:752–759

Hamblin MW, McGuffin RW, Metcalf MA, Dorsa DM, Merchant KM (1992b) Distinct 5-HT_{1B} and 5-HT_{1D} receptors in rat: structural and pharmacological comparison of the two cloned receptors. Mol Cell Neurosci 3:578–587

Hartig PR (1989) Molecular Biology of 5-HT receptors. Trends Pharmacol Sci 10:64–69

Hartig PR, Branchek TA, Weinshank, RL (1992) A subfamily of 5-HT_{1D} receptor genes. Trends Pharmacol Sci 13:152–159

Herrick-Davis K, Titeler M (1988) Detection and characterization of the serotonin 5-HT_{1D} receptor in rat and human brain. J Neurochem 50:1624–1631

Heuring RJ, Peroutka SJ (1987) Characterization of a novel ^{3}H-5-hydroxytryptamine binding site subtype in bovine brain membranes. J Neurosci 7:894–903

Hong JS, Yang H-YT, Racagni G, Costa E (1977) Projections of substance P containing neurons from neostriatum to substantia nigra. Brain Res 122:541–544

Hoyer D (1991) The 5-HT receptor family: ligands, distribution and receptor-effector coupling. In: Rodgers RJ, Cooper SJ (eds) 5-HT_{1A} agonists, 5-HT_3 antagonists and benzodiazepines: their comparative behavioural pharmacology. Wiley, Chichester, pp 31–57

Hoyer D, Engel G, Kalkman HO (1985) Characterization of the 5-HT_{1B} recognition site in rat brain: binding studies with [^{125}I]iodocyanopindolol. Eur J Pharmacol 118:1–12

Hoyer D, Lery H, Nozulak J, Palacios JM, Bruinvels AT (1992) '5-HT_{1R}' or 5-HT_{1D} binding? Evidence for 5-HT_{1D} binding in rabbit brain. Naunyn-Schmiedeberg's Arch Pharmacol 346:249–255

Hoyer D, Middlemiss DN (1989) The pharmacology of the terminal 5-HT autoreceptors in mammalian brain: evidence for species differences. Trends Pharmacol Sci 10:130–132

Hoyer D, Schoeffter P (1988) 5-HT_{1D} receptors inhibit forskolin-stimulated adenylate cyclase activity in calf substantia nigra. Eur J Pharmacol 147:145–147

Jin H, Oksenberg D, Askenazi A, Peroutka SJ, Duncan AMV, Rozmahel R, Yang Y, Mengod G, Palacios JM, O'Dowd BF (1992) Characterization of the human 5-hydroxytryptamine$_{1B}$ receptor. J Biol Chem 267:5735–5738

Levy FO, Gudermann T, Birnbaumer M, Kaumann AJ, Birnbaumer L (1992) Molecular cloning of a human gene (S31) encoding a novel serotonin receptor mediating inhibition of adenylyl cyclase. FEBS Lett 296:201–206

Limberger N, Deicher R, Starke K (1991) Species differences in presynaptic serotonin autoreceptors: mainly 5-HT_{1B} but possibly in addition 5-HT_{1D} in the rat, 5-HT_{1D} in the rabbit and guinea-pig brain cortex. Naunyn-Schmiedeberg's Arch Pharmacol 343: 353–364

Macor JE, Burkhart CA, Heym JH, Ives JL, Lebel LA, Newman ME, Nielsen JA, Ryan K, Schulz DW, Torgersen LK, Koe BK (1990) 3-(1,2,5,6-tetrahydropyrid-4-yl)pyrrolo[3, 2-b]pyrid-5-one a potent

and selective serotonin 5-HT_{1B} agonist and rotationally restricted phenolic analogue of 5 methoxy-3-(1,2,5,6-tetrahydropyrid-4-yl)indole. J Med Chem 33:2087–2093

Maroteaux L, Saudou F, Amlaiky N, Boschert U, Plassat JL, Hen R (1992) The mouse $5HT_{1B}$ serotonin receptor: cloning, functional expression and localisation in motor control centers. Proc Natl Acad Sci USA 89:3020–3024

Maura G, Raiteri M (1986) Cholinergic terminals in rat hippocampus possess 5-HT_{1B} receptors mediating inhibition of acetycholine release. Eur J Pharmacol 129:333–337

Maura G, Roccatagliata E, Raiteri M (1986) Serotonin autoreceptor in rat hippocampus: Pharmacological characterization as a subtype of the 5-HT_1 receptor. Naunyn-Schmiedeberg's Arch Pharmacol 334:323–326

McAllister G, Charlesworth A, Snodin C, Beer MS, Noble AJ, Middlemiss DN, Iversen LL, Whiting P (1992) Molecular cloning of a serotonin receptor from human brain (5-HT1E): a fifth 5-HT1-like subtype. Proc Natl Acad Sci USA 89:5517–5521

Middlemiss DN, Bremer ME, Smith SM (1988) A pharmacological analysis of the 5-HT receptors mediating inhibition of 5-HT release in the guinea-pig frontal cortex. Eur J Pharmacol 157:101–107

Palacios JM, Waeber C, Bruinvels AT, Hoyer D (1992) Direct visualization of $serotonin_{1D}$ receptors in the human brain using a new radioiodinated radioligand. Mol Brain Res 13:175–179

Pazos A, Palacios JM (1985) Quantitative auto- radiographic mapping of serotonin receptors in the rat brain. I. Serotonin-1 receptors. Brain Res 346:205–230

Pazos A, Engel G, Palacios JM (1985) Beta-adrenoreceptor blocking agents recognize a subpopulation of serotonin receptors in brain. Brain Res 343:403–408

Pedigo NW, Yamamura HI, Nelson DL (1981) Discrimination of multiple [^{3}H]5-hydroxytryptamine-binding sites by the neuroleptic spiperone in rat brain. J Neurochem 36:220–226

Peroutka SJ (1988) 5-Hydroxytryptamine receptor subtypes: Molecular, biochemical and physiological characterization. Trends Neurosci 11:496–499

Peroutka SJ, Snyder SH (1979) Multiple serotonin receptors: differential binding of [^{3}H]5-hydroxytryptamine, [^{3}H]lysergic acid diethylamide and [^{3}H]spiroperidol. Mol Pharmacol 16:687–699

Ribak CE, Vaughn JE, Roberts E (1980) GABAergic nerve terminals decrease in substantia nigra following hemitransections of striatonigral and pallidonigral pathways. Brain Res 192:413–420

Schipper J, Tulp MTM (1988) Serotonin autoreceptors in guinea pig cortex slices resemble the 5-HT_{1D} binding site. Soc Neurosci Abstr 14:552

Schlicker E, Fink K, Göthert M, Hoyer D, Molderings G, Roschke I, Schoeffter P (1989) The pharmacological properties of the presynaptic serotonin autoreceptor in the pig brain cortex conform to the 5-HT_{1D} receptor subtype. Naunyn-Schmiedeberg's Arch Pharmacol 340:45–51

Schoeffter P, Hoyer D (1989) 5-Hydroxytryptamine 5-HT_{1B} and 5-HT_{1D} receptors mediating inhibition of adenylate cyclase activity pharmacological comparison with special reference to the effects of yohimbine rauwolscine and some beta-adrenoceptor antagonists. Naunyn-Schmeideberg's Arch Pharmacol 340:285–292

Sijbesma H, Schipper J, Cornelissen JCHM, De Kloet ER (1991) Species differences in the distribution of central 5-HT_1 binding sites a comparative autoradiographic study between rat and guinea-pig. Brain Res 555:295–304

Vergé D, Daval G, Marcinkiewicz M, Patey A, El Mestikawy S, Gozlan H, Hamon M (1986) Quantitative autoradiography of multiple 5-HT1 receptor subtypes in the brain of control or 5,7-dihydroxytryptamine-treated rats. J Neurosci 6:3474–3482

Voigt MM, Laurie DJ, Seeburg PH, Bach A (1991) Molecular cloning and characterization of a rat brain cDNA encoding a 5-hydroxytryptamine 1B receptor. EMBO J 10:4017–4023

Waeber C, Palacios JM (1992) Autoradiographic evidence that non 5-HT_{1A}/5-HT_{1C} [^{3}H]5-HT binding sites are of the 5-HT_{1B} subtype in the hamster and opossum brain, of the 5-HT_{1D} subtype in the rabbit brain. Synapse 12:261–270

Waeber C, Schoeffter P, Palacios JM, Hoyer D (1988) Molecular pharmacology of 5-HT_{1D} recognition sites: radioligand binding studies in human, pig and calf brain membranes. Naunyn Schmiedeberg's Arch Pharmacol 337:595–601

Waeber C, Dietl MM, Hoyer D, Palacios JM (1989a) 5-HT_1 receptors in the vertebrate brain. Regional distribution examined by autoradiography. Naunyn-Schmiedeberg's Arch Pharmacol 340:486–494

Waeber C, Schoeffter P, Palacios JM, Hoyer D (1989b) 5- HT(1D) receptors in guinea-pig and pigeon brain. Radioligand binding and biochemical studies. Naunyn-Schmiedeberg's Arch Pharmacol 340:479–485

Weinshank RL, Zgombick JM, Macchi M, Branchek TA, Hartig PR (1992) Human serotonin 1D receptor is encoded by a subfamily of two distinct genes: 5-$HT_{1D\alpha}$ and 5-$HT_{1D\beta}$. Proc Natl Acad Sci USA 89:3630–3634

Zarbin MA, Palacios JM, Wamsley JK, Kuhar MJ (1983) Axonal transport of beta-adrenergic receptors: antero- and retrogradely transported receptors differ in agonist affinity and nucleotide sensitivity. Mol Pharmacol 24:341–348